A Molecular Dynamics Simulation Study of the Influence of Hydrogen-Bonding and Polar Interactions on Hydration and Conformations of a Poly(ethylene oxide) Oligomer in Dilute Aqueous Solution

Grant D. Smith* and Dmitry Bedrov

Department of Materials Science and Engineering and Department of Chemical and Fuels Engineering, 122 S. Central Campus Drive, Rm. 304, University of Utah, Salt Lake City, Utah 84112

Received June 15, 2001
Revised Manuscript Received April 29, 2002

I. Introduction

While molecular simulations, such as our recent study of the influence of solution composition and temperature on hydrogen bonding in aqueous poly(ethylene oxide) (PEO) solutions,[1] as well as numerous experimental investigations,[2] have provided valuable insight into the thermodynamics and structural properties of aqueous polymer solutions, a fundamental understanding of the role of water−polymer interactions on conformations and solution thermodynamics of amphiphilic polymers such as PEO and proteins remains elusive. Here we report on a molecular dynamics (MD) simulation study of the influence of polymer−water hydrogen bonding and polar interactions on the solvation thermodynamics, hydration structure, and conformations of aqueous solutions of 1,2-dimethoxyethane (DME), a model compound (dimer) for PEO. We first compare the conformations and hydration structure in PEO and DME solutions in order to establish that DME is a good model compound for PEO, i.e., that the aqueous solvation (or hydration) of DME closely resembles that of PEO. Next, we investigate in detail the hydration thermodynamics for DME in dilute aqueous solution, specifically the influence of ether−water hydrogen bonding and ether−water polar interactions on the excess free energy, enthalpy, and entropy of solution as well as the influence of these interactions on water−water interactions, the structure of hydrating water, and the conformations of the ether.

II. Comparison of Conformations and Hydration in PEO and DME Solutions

For the purposes of comparing conformations and hydration in PEO and DME aqueous solutions, we have performed MD simulations on solutions of PEO-12 (H−$[CH_2-O-CH_2]_{12}$−H, MW = 530 Da) and DME (H−$[CH_2-O-CH_2]_2$−H, MW = 90 Da) at compositions w_p (weight fraction of polymer) = 0.025, 0.17, 0.35, 0.52, 0.65, 0.78, 0.9, and 1.0 using the methodology described in detail elsewhere.[3] These simulations were performed at 318 K in an NVT ensemble at densities yielding an average pressure P = 1 atm for each composition. Quantum chemistry based potentials described elsewhere were employed for the polymer[4] as well as polymer−water interactions,[5] and the TIP4P potential[6] was used for water. The systems consisted of 1−32 polymer molecules with 1152−100 water molecules and 1−72 DME molecules with 500−28 water molecules, depending upon composition.

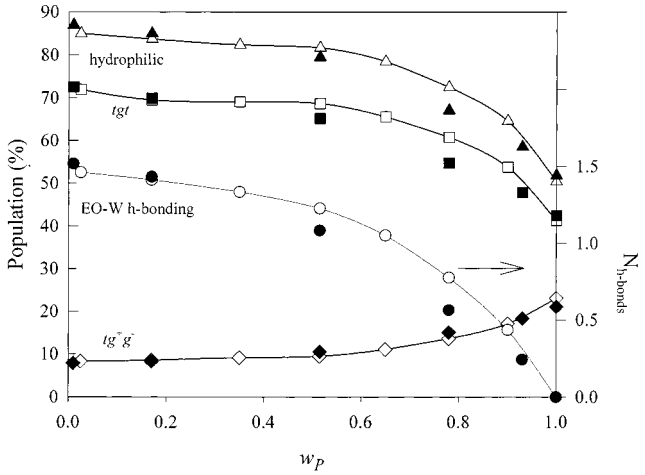

Figure 1. Total hydrophilic conformer population, populations of the most important hydrophilic and hydrophobic conformers, and number of ether−water hydrogen bonds per ether oxygen for DME (open symbols) and PEO (closed symbols) in aqueous solution as a function of composition (w_p).

Local PEO and DME conformations can be classified as hydrophilic or hydrophobic on the basis of their change in population upon hydration.[1] The C−O−C−C−O−C *tgt* and *tgg* triad conformer populations increase (compared to the gas phase or neat melt) upon hydration while all other major conformer populations (*ttt*, *ttg*, tg^+g^-) decrease. The total populations of hydrophilic conformers in PEO and DME solutions as well as the populations of the principal hydrophilic (*tgt*) and hydrophobic (tg^+g^-) conformers are compared as a function of solution composition in Figure 1. As reported previously, the hydrophilic conformer population increases with dilution for PEO[7] and its oligomers.[8,9] The similarity in conformer populations for PEO and DME and their dependence on solution composition indicates that DME in aqueous solution has essentially the same local conformations as PEO.

Similarity in hydration of PEO and DME is illustrated in Figure 2 where the ether oxygen (O_e)−water oxygen (O_w) pair distribution functions $g(r)$ are shown for selected solution compositions. The positions of the first, second, and third maxima correspond almost exactly for the PEO and DME solutions. The composition dependence of the first maxima, which involves primarily water molecules that are hydrogen bonded to PEO and DME, is very similar for the two solutions. For the second and third maxima, we see a decrease in the peak height with dilution for the PEO solutions that is not reproduced in the DME solutions. This difference is due to the exclusion of several water molecules in dilute solution from the vicinity of any given PEO ether oxygen by neighboring repeat units. Considering an ether−water hydrogen bond to exist whenever the O_e-H_w (water hydrogen) distance is less than 2.675 Å,[1] we have also calculated the number of ether−water hydrogen bonds ($N_{h-bonds}$) per ether oxygen atom for both PEO and DME solutions, as shown in Figure 1. The extent of ether−water hydrogen bonding and its composition dependence are quite similar for PEO and DME solutions, largely saturating with dilution at $w_p \approx 0.50$ as reported previously.[1] The somewhat greater extent of ether−water hydrogen bonding in the more concen-

10.1021/ma011026t CCC: $22.00
Published on Web 06/07/2002

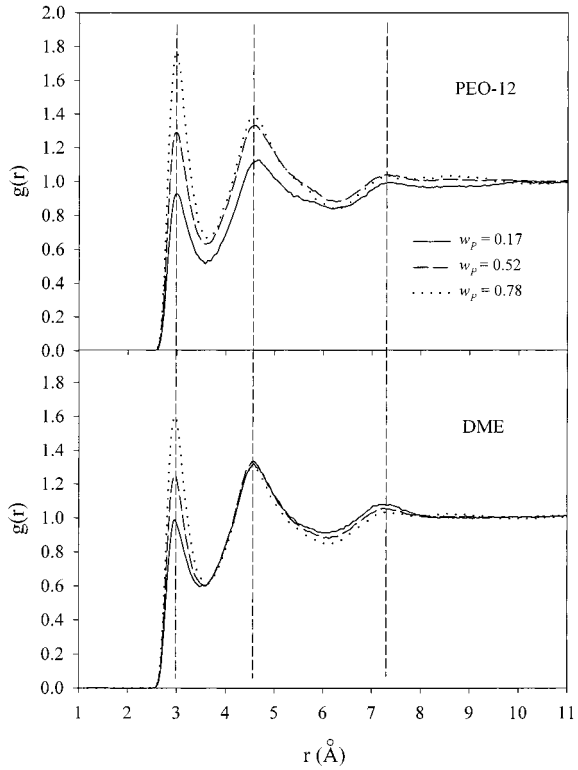

Figure 2. Ether oxygen−water oxygen pair distribution functions for aqueous DME and PEO solutions for several solution compositions at 318 K. Vertical lines illustrate the correspondence of the positions of the structural peaks.

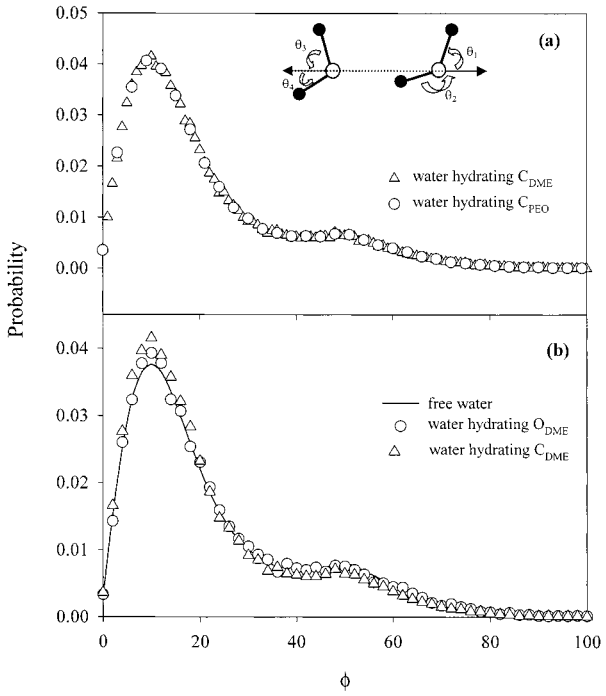

Figure 3. Water−water hydrogen bond angle distribution for (a) water hydrating ether carbon atoms for aqueous DME and PEO solutions and (b) bulk (free) water, water hydrating ether oxygen, and water hydrating ether carbon atoms for an aqueous DME solution, at 318 K and w_p = 0.17. The inset shows the four hydrogen-bonding angles for a water pair, the smallest of which is used in determining the distributions.

trated PEO solutions compared to the corresponding DME solutions is due to the increased tendency of a water molecule to form multiple hydrogen bonds with the same PEO molecule when there is a paucity of water.[1]

Finally, in Figure 3 we show the distribution of hydrogen bond angles O_w- - -O_w−H_w (where - - - indicates a hydrogen bond, see inset of Figure 3) for bulk water, water hydrating ether carbon atoms, and water hydrating ether oxygen atoms for PEO and DME solutions at w_p = 0.17. The distribution shown is for the smallest of the four O- - -O−H angles formed by a water molecule and each coordinating water molecule, defined as all waters such that the O_w- - -O_w distance is <3.4 Å. Figure 3a reveals that carboneous hydration, quantified by the distribution of hydrogen bond angles formed by all water molecules such that the O_w- - -C_e (ether carbon) distance is <4.2 Å with their coordinating water molecules, is nearly identical for the PEO and DME solution, as is the oxygeneous hydration involving water molecules such that the O_w- - -O_e distance is <3.6 Å (not shown). Figure 3b reveals that oxygeneous hydration of DME (and hence PEO) is hydrophilic in that the distribution of hydrogen bond angles for water hydrating the ether oxygen atoms is quite similar to that for bulk water. However, water involved in carboneous hydration shows an increased probability of smaller water−water hydrogen-bonding angles indicative of greater icelike structure and hence hydrophobic hydration.[10]

III. Influence of Ether−Water Hydrogen-Bonding and Polar Interactions on Hydration Thermodynamics

Figures 1−3 clearly demonstrate that the conformations, extent of ether−water hydrogen bonding, and the structure of hydrating water as a function of composition are very similar for DME and PEO solutions, establishing DME as an excellent model for PEO for purpose of investigating of the influence of ether−water hydrogen-bonding and polar interactions on local conformations and hydration. The use of DME as a model compound for PEO is further justified by the fact that it is possible to utilize the self-consistent histogram method[11−13] in determining the free energy of hydration of DME, as was done in our previous work,[3,5] while such computations would be prohibitively expensive for higher molecular weight PEO. Therefore, we have carried out simulations of a single DME molecule with 500 water molecules at 298 K for the purpose of elucidating the influence of hydrogen-bonding and polar interactions on hydration thermodynamics, structure, and conformations of our PEO model compound. In future papers we will report on the hydration thermodynamics of PEO model compounds as a function of concentration, temperature, and molecular weight.

Free Energy Calculations. In our potential[5] ether−water hydrogen bonds are engendered primarily by electrostatic interactions represented by partial atomic charges. However, we found that an improved description of ether−water binding obtained from high-level quantum chemistry calculations as well as improved agreement with experiment for the excess volume, Gibbs free energy, and enthalpy of solvation for DME in water could be obtained by inclusion of an additional, specific short-range interaction between ether oxygen and water hydrogen atoms,[5] given by

$$E_{HB}(r_{Oe-Hw}) = -60.2 \exp(-2.0 r_{Oe-Hw}) \qquad (1)$$

where E_{HB} is the energy of the hydrogen-bonding

Table 1. Excess Properties for Dilute DME/Water Solutions at 298 K

property (kcal/mol)	unperturbed[a]	nonpolar[b]	polar w/o h-bonds[b]	DME expt[c]	pentane expt[c,d]
ΔG_{EX}	−6.2	+0.5 (6.7)	−2.4 (3.8)	−4.8	2.3 (7.1)
ΔH_{EX}	−17.1	−9.4 (7.7)	−11.9 (4.9)	−14.2	−5.9 (7.9)
$T\Delta S_{EX}$	−10.9	−10.0 (0.9)	−9.6 (1.0)	−9.4	−8.2 (0.8)

[a] From ref 5. [b] Values in parentheses are relative to the unperturbed solution. [c] From ref 14. [d] Values in parentheses are relative to DME (experimental).

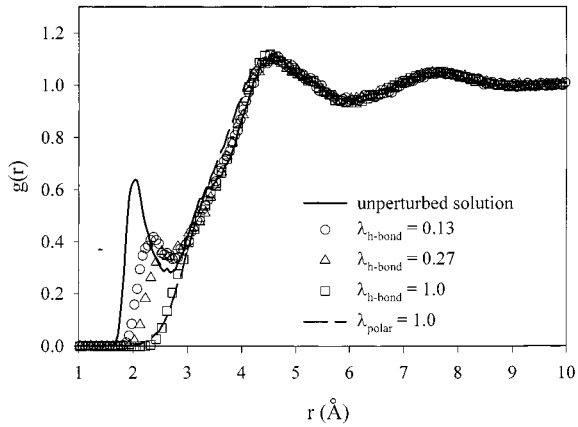

Figure 4. Ether oxygen−water hydrogen pair distribution functions for dilute DME solution at 298 K for various values of interaction scaling parameter λ.

function (in kcal/mol) and r_{Oe-Hw} is the ether oxygen−water hydrogen separation (in Å). In our previous work[5] we employed the self-consistent multiple histogram method[11−13] to determine the free energy associated with solvation (hydration) of a single DME molecule in water using this potential. In that work we obtained a value of $\Delta G_{EX} = -6.2$ kcal/mol and a value of $\Delta H_{EX} = -17.1$ kcal/mol relative to pure water and gas-phase DME at 298 K, in good agreement with experimental values[14,15] for the Gibbs free energy and enthalpy of hydration, as shown in Table 1.

To examine the influence of ether−water hydrogen bonding on the thermodynamics of ether solvation, the structure of hydrating water, and the conformations of the ether, we again employed the self-consistent histogram technique used to obtain the free energy of DME hydration but introduced an additional energy function of the form

$$E(r_{Oe-Hw}) = \lambda_{h-bond}[23474 \exp(-3.74 r_{Oe-Hw})] \quad (2)$$

This short-range function was parametrized so as to reduce the number of water hydrogen atoms in the first coordination shell of an ether oxygen atom (and hence ether−water hydrogen bonding) while leaving O_e- - -H_w coordination relatively unperturbed at larger distances, as shown in Figure 4. Simulations were performed with Hamiltonians corresponding to $0.0 \le \lambda_{h-bond} \le 1$. In all histogram and energy analyses of the simulation trajectories the energy associated with this anti-hydrogen-bonding function was subtracted from the total potential energy.

Similarly, the influence of polar (electrostatic) ether−water interactions on solution thermodynamics and hydration structure was studied by performing a series of simulations where these interactions were scaled by a factor λ_{polar}, yielding ether−water Coulomb interactions of the form

$$E_{ij}(r_{ij}) = (1 - \lambda_{polar})332.1 q_i q_j / r_{ij} \quad (3)$$

where q_i is the partial atomic charge on an ether atom and q_j is the partial atomic charge on a water atom. This scaling factor was also applied to the specific ether−water hydrogen bonding function, eq 1, yielding

$$E_{HB}(r_{Oe-Hw}) = (1 - \lambda_{polar})[-60.2 \exp(-2.0 r_{Oe-Hw})] \quad (4)$$

as we consider this contribution to the ether−water binding to be primarily an electrostatic interaction that is not well represented by fixed partial atomic charges.[5] Again, simulations were performed using Hamiltonians corresponding to $0.0 \le \lambda_{polar} \le 1.0$. Note that a value of $\lambda_{polar} = 1.0$ corresponds to nonpolar ether−water interactions and that the *intramolecular* ether potential and water−water potential are not influenced by either of the perturbing potentials (eq 2 or eqs 3 and 4).

All simulations were carried out in the NVT ensemble at a density corresponding to $P = 1$ atm for the unperturbed solution. Helmholtz free energies relative to the unperturbed solution for all values of λ_{h-bond} and λ_{polar} were determined using the self-consistent histogram method. The internal energy of the solution relative to the unperturbed solution was determined directly from ensemble averages. Conversion to the NPT ensemble at $P = 1$ atm was carried out by utilizing an equation of state for the DME/water solution determined by conducting simulations of the unperturbed solution at several fixed volumes and fitting the solution energy and pressure as linear functions of volume. The solution volume for each λ_{h-bond} and λ_{polar} corresponding to $P = 1$ atm was obtained utilizing the equation of state for the unperturbed solution. The solution energy at each λ_{h-bond} and λ_{polar} was then corrected according to the corresponding volume change. The validity of this equation-of-state approach was confirmed by performing NPT simulations for $\lambda_{h-bond} = 1$ and $\lambda_{polar} = 1$, which yielded the same solution volumes and energies obtained by making equation-of-state corrections to the NVT values. The Helmholtz free energy was corrected for volume change at constant temperature using the relationship

$$\Delta A = -\int_{V_1}^{V_2} P(V)\, dV \quad (5)$$

where the volume-dependent pressure $P(V)$ is given by the equation of state described above. For all values of λ_{h-bond} and λ_{polar} the volume correction to the Helmholtz free energy was negligible. Finally, the Gibbs free energy ΔG and enthalpy ΔH relative to the unperturbed solution for all values of λ_{h-bond} and λ_{polar} were determined from the corresponding volume-corrected Helmholtz free energies and internal energies by addition of the $P\Delta V$ term, with change in entropy given by $T\Delta S = \Delta H - \Delta G$. Since $P = 1$ atm and the volume change was small for all λ_{h-bond} and λ_{polar} (increasing slightly with λ), $P\Delta V$ was negligible for all cases.

Extent of Hydrogen Bonding. The number of ether−water hydrogen bonds per ether oxygen ($N_{h-bonds}$) and the effective ether dipole moment (μ_{DME}) are shown in Figure 5a as a function of λ_{polar} and λ_{h-bond}. The effective average dipole moment of DME is given as $\mu_{DME} = (1 - \lambda_{polar})\langle|\sum q_i \mathbf{r}_i|\rangle$ where the sum is over all atoms of a DME molecule. With increasing perturbation (λ_{h-bond} or $\lambda_{polar} > 0$) the extent of ether−water hydrogen

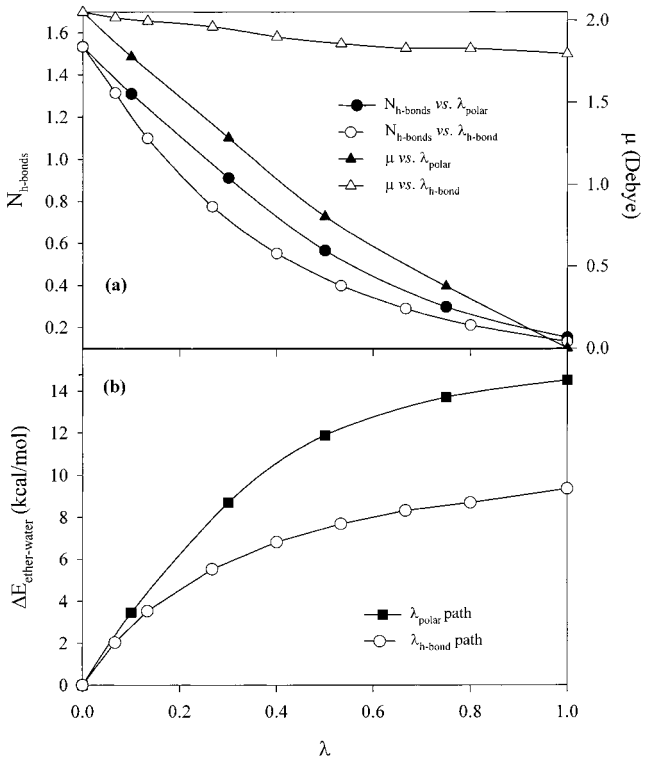

Figure 5. Number of ether−water hydrogen bonds per ether oxygen and the dipole moment of DME (a) as well as ether water energy ($\Delta E_{ether-water}$) (b) as a function of the interaction scaling parameter λ at 298 K.

bonding and the dipole moment of DME decrease. We consider $N_{h-bonds} = 0.15$, corresponding to the residual level of ether−water hydrogen bonding in solutions with nonpolar ($\lambda_{polar} = 1.0$) ether−water interactions to correspond to complete destruction of ether−water hydrogen bonding. This same extent of ether−water hydrogen bonding occurs in solutions with $\lambda_{h-bond} \approx 1.0$. Figure 4 shows that the O_e-H_w pair distribution functions for $\lambda_{polar} = 1.0$ (nonpolar ether−water interactions) and $\lambda_{h-bond} = 1.0$ (non-hydrogen-bonding ether water interactions) are quite similar. Note that λ_{h-bond} has relatively little influence on the effective DME dipole moment since $\lambda_{polar} = 0.0$ for the λ_{h-bond} path, and hence the only change in the average dipole moment of DME is due to changing conformational populations. Therefore, $\lambda_{h-bond} \approx 1.0$ corresponds to a solution with large polar ether−water interactions but without ether−water hydrogen bonds.

Hydration Thermodynamics. Figure 5b shows the change in the average ether−water interaction energy relative to the unperturbed solution ($\lambda_{polar} = \lambda_{h-bond} = 0$), $\Delta E_{ether-water}$, as a function of λ_{h-bond} and λ_{polar}. As expected, the ether−water energy becomes monotonically less favorable with increasing λ_{h-bond} and λ_{polar}. Reasonably, the solution with completely nonpolar DME−water interactions ($\lambda_{polar} = 1.0$) has less favorable ether−water interactions than the solution without ether−water hydrogen bonding but with non-hydrogen-bonding polar interactions ($\lambda_{h-bond} = 1.0$). We found $\Delta E_{ether-water}$, which is a measure of the influence of the perturbing potential (λ_{h-bond} or λ_{polar}) on ether−water interactions, to be a convenient parametric variable for comparing the influence of ether−water hydrogen-bonding and ether−water polar interactions on the thermodynamics of DME hydration, as described below.

Figure 6a reveals that as ether−water polar interactions are scaled down by increasing λ_{polar}, the Gibbs free energy of solvation of DME relative to the unperturbed solution, ΔG, increases directly with $\Delta E_{ether-water}$. For the solution with nonpolar ($\lambda_{polar} = 1.0$) ether−water interactions the free energy of hydration is about 6.7 kcal/mol less favorable than for polar (unperturbed) DME. Hence, as summarized in Table 1, polar interactions, which include implicitly hydrogen-bonding effects, account for all of the favorable (−6.2 kcal/mol) excess Gibbs free energy of DME hydration: nonpolar DME ($\lambda_{polar} = 1.0$) has a small positive (−6.2 kcal/mol + 6.7 kcal/mol = 0.5 kcal/mol) excess free energy of hydration. Eliminating ether−water hydrogen bonds while maintaining ether−water polar interactions ($\lambda_{h-bond} > 0$) results in a solution free energy that increases less rapidly with $\Delta E_{ether-water}$ than occurs when all DME−water polar interactions are scaled down. This less dramatic increase in ΔG, particularly for small $\Delta E_{ether-water}$, is due to an increase in entropy associated with destruction of the ether−water hydrogen bonds, as well as a larger negative contribution to the change in solution energy resulting from stronger water−water interactions, as discussed below. Complete destruction of ether−water hydrogen bonds ($\lambda_{h-bond} = 1.0$) yields a free energy of hydration about 3.8 kcal/mol less favorable than for the fully interacting ether−water solution (see Table 1). Hence, about 60% of the −6.7 kcal/mol of the excess Gibbs free energy of hydration of DME that can be associated with electrostatic interactions between water and the ether is due to ether−water hydrogen-bonding interactions and the remainder to non-hydrogen-bonding polar interactions.

Figure 6b reveals that the enthalpy of hydration ΔH, relative to the unperturbed solution, increases more or less proportionally to $\Delta E_{ether-water}$ with decreasing extent of ether−water hydrogen-bonding and ether−water polar interactions. We can associate about −7.7 kcal/mol of the excess ether hydration enthalpy ΔH_{EX} with electrostatic effects or almost $^1/_2$ of the total for the unperturbed solution (see Table 1). Of this, −4.9 kcal/mol, or about 60%, is associated with ether−water hydrogen bonding. Since DME has two ether oxygen atoms, and $N_{h-bonds}$ is reduced from about 1.5 ($\lambda_{h-bond} = 0$) to about 0.15 ($\lambda_{h-bond} = 1.0$) along the λ_{h-bond} path as shown in Figure 5a, this process can be associated with the destruction of about 2.7 hydrogen bonds. An energy of $-4.9/2.7 = -1.8$ kcal/mol for an ether−water hydrogen bond is somewhat less than the value of −3.5 to −4 kcal/mol that has been discerned from NMR relaxation time measurements[16] and subsequently used in a recent theoretical model for PEO/water solutions.[17] A similar value was obtained from our recent simulation study of the temperature dependence of PEO−water hydrogen bonding.[1] However, the energy associated with breaking an ether−water hydrogen bond in these studies is probably more closely related to the change in ether−water energy than the change in total solution energy. The dashed curve in Figure 6b corresponds to $\Delta H = \Delta E_{ether-water}$. Clearly, the increase in solution enthalpy (and hence energy, as $P\Delta V$ effects are negligible) associated with breaking ether−water hydrogen bonds and reducing ether−water polar interactions is smaller than the increase in ether−water energy, indicating that reducing the extent of ether−water hydrogen bonds or decreasing the effective dipole moment of DME results in stronger water−water interac-

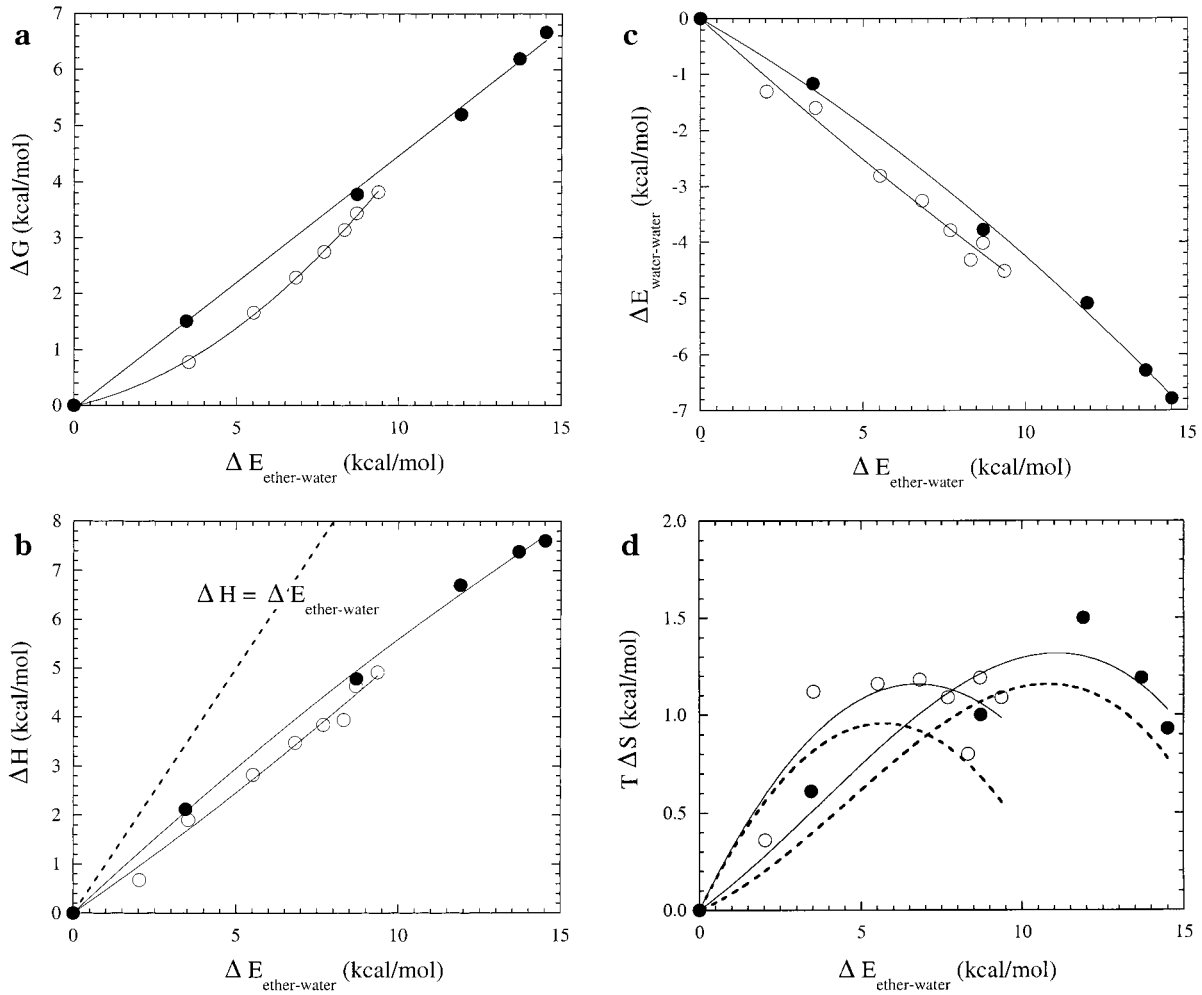

Figure 6. Change in thermodynamic properties of the dilute ether−water solution at 298 K as a function of the parametric variable $\Delta E_{\text{ether-water}}$ relative to the unperturbed solution. (See Figure 5b for the relationship between $\Delta E_{\text{ether-water}}$ and the scaling parameters $\lambda_{\text{h-bond}}$ and λ_{polar}.) (a) ΔG = Gibbs free energy, (b) ΔH = enthalpy, (c) $\Delta E_{\text{water-water}}$ = water−water energy, and (d) $T\Delta S$ = entropy. Open symbols are for $\lambda_{\text{h-bond}}$, and closed symbols are for λ_{polar}. Solid lines serve to guide the eye. Also shown in (d) is the change in solution entropy after subtraction of translational entropy effects due to differences in solution volume (dash lines without symbols).

tions. This effect is illustrated in Figure 6c, where it can be seen that the water−water interactions become stronger more or less proportionally to $\Delta E_{\text{ether-water}}$. For the same $\Delta E_{\text{ether-water}}$ the increase in water−water interactions is somewhat greater for the $\lambda_{\text{h-bond}}$ path than for the λ_{polar} path, accounting for the slower rise in ΔH (Figure 6b) and partially for the slower rise in ΔG (Figure 6a) for the $\lambda_{\text{h-bond}}$ path with $\Delta E_{\text{ether-water}}$. The strengthening of water−water interactions as the ether−water interactions become more hydrophobic (i.e., as ΔG and ΔH increase) is also reflected in increased structuring of the hydrating water, as discussed below. If we consider only the change in ether−water energy upon destruction of ether−water hydrogen bonds ($\lambda_{\text{h-bond}} = 1.0$), we obtain a value (see Figure 5b) of $-9.4/2.7 = -3.5$ kcal/mol for an ether−water hydrogen bond, in good agreement with previous estimates.[1,16,17]

Finally, the change in the entropy of solvation relative to the unperturbed DME solution as a function of $\Delta E_{\text{ether-water}}$ is illustrated in Figure 6d. A decrease in ether−water hydrogen-bonding or ether−water electrostatic interactions initially results in an increase in solution entropy, indicating that the destruction of ether−water hydrogen bonds and ether−water polar interactions is energetically unfavorable (Figure 6b) but entropically favorable. This is consistent with the entropy of formation of ether−water hydrogen bonds determined from the temperature dependence of ether−water hydrogen bonding in PEO solutions in our previous simulations.[1] The initial increase in entropy is greater for the $\lambda_{\text{h-bond}}$ path, accounting in part for the slower rise in ΔG with $\Delta E_{\text{ether-water}}$ seen in Figure 6a. After subtracting the increase in translational entropy due to the small increase in solution volume with λ from the total entropy change,[18] both the $\lambda_{\text{h-bond}}$ and λ_{polar} paths exhibit a maximum in entropy corresponding to about $N_{\text{h-bonds}} \approx 0.6-0.7$. For larger λ values the increasingly hydrophobic character of the water−DME interactions (see below) is reflected in a decrease in solution entropy.[19] When the ether−water interactions become completely nonpolar ($\lambda_{\text{polar}} = 1.0$) or all ether−water hydrogen bonds have been destroyed ($\lambda_{\text{h-bond}} = 1.0$), much of the entropy gained by the removal of ether−water hydrogen bonds and restrictions on water orientation due to ether−water polar interactions has been lost due to greater hydrophobic structuring of the hydrating water. A consequence of the offsetting of gains in solution entropy due to weaker ether−water interactions by a loss in entropy resulting from increased water structuring associated with more hydrophobic ether−

water interactions is a small net influence of hydrogen-bonding and electrostatic interactions on solution entropy. Hence, the influence of ether−water hydrogen-bonding and polar interactions on the solvation entropy is quite small compared to the total excess entropy of solvation as well as the influence of these interactions on the excess free energy and enthalpy, as summarized in Table 1.

Finally, it can be seen in Table 1 that the excess free energy, enthalpy, and entropy of hydration for nonpolar DME ($\lambda_{polar} = 1.0$) are in good agreement with experimental values for pentane, which has nearly the same molar volume as DME. Furthermore, the difference in the free energy, enthalpy, and entropy of hydration between nonpolar and unperturbed DME from simulation is nearly identical to the corresponding difference between pentane and DME obtained from experiment. These correspondences strongly support the accuracy of our potential function as well as the accuracy of the changes in the free energy, enthalpy, and entropy of hydration predicted as a function of ether−water polar interactions.

IV. Influence of Ether−Water Interactions on the Structure of Hydrating Water

The (cumulative) probability for water−water hydrogen bonds with an angle ≤30° (icelike hydrogen bonding) for water in the first hydration shell of DME is a useful measure of the relative extent of water structuring.[10] This cumulative probability was determined from distributions such as shown in Figure 3 for DME water solutions as a function of λ_{h-bond} and λ_{polar} for bulk, carboneous, and oxygeneous water (see section II for definitions) and is shown in Figure 7 as a function of $\Delta E_{ether-water}$. Also shown in Figure 7 is the water coordination number N_w for carboneous and oxygeneous water molecules which is a measure of the extent of water−water interactions. Figure 7 reveals that the structure of the carboneous water as measured by the probability of icelike water−water hydrogen bonds as well N_w is unaffected by the increasing hydrophobic character of the ether−water interactions with decreasing ether−water hydrogen-bonding or polar interactions. However, the oxygeneous water shows a dramatic increase in water coordination number and increased icelike structuring. The increasing extent of water−water interaction with increasing ether hydrophobicity indicated by the water−water energy (Figure 6c) therefore appears to involve primarily oxygeneous water molecules, whose extent of water−water hydrogen bonding approaches that of carboneous waters for large values of λ. Hence, the entropy gained by removal of restrictions on water through elimination of ether−water hydrogen bonds or polar interactions between the water and ether is largely offset by entropy loss associated with additional structuring of the oxygeneous water. The water coordination number and extent of icelike hydrogen bonding for oxygeneous waters increase more rapidly with $\Delta E_{ether-water}$ for the λ_{h-bond} path than for the λ_{polar} path, consistent with the greater reduction in water−water energy for this path (Figure 6c).

V. The Role of Conformations in PEO Hydration

Finally, we investigated the relative hydration thermodynamics of hydrophilic and hydrophobic DME conformers and the influence of ether−water hydrogen-bonding and polar interactions on DME conformer

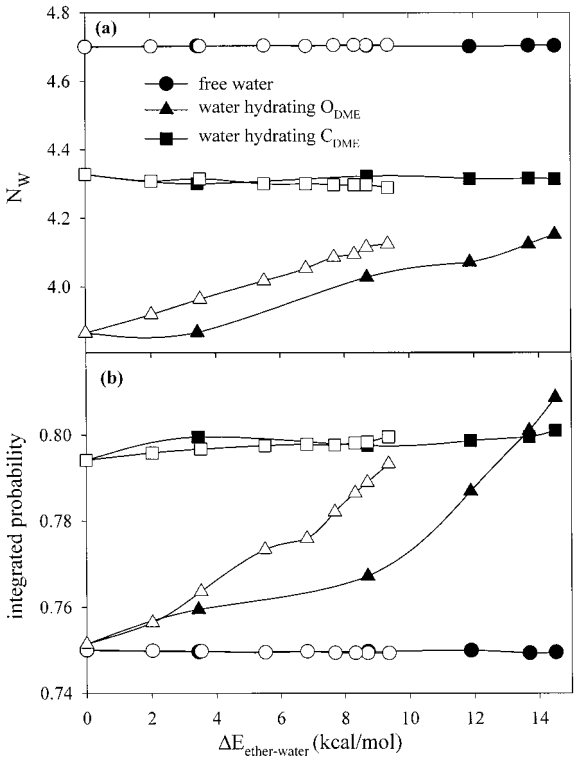

Figure 7. Cumulative probability for low-angle (<30°) icelike water−water hydrogen bonds for bulk waters, oxygeneous water, and carboneous water as a function of the parametric variable $\Delta E_{ether-water}$ (a). Also shown is the number of water molecules in the first hydration shell of the various types of water (b). Open symbols are for λ_{h-bond}, and closed symbols are for λ_{polar}. Solid lines serve to guide the eye.

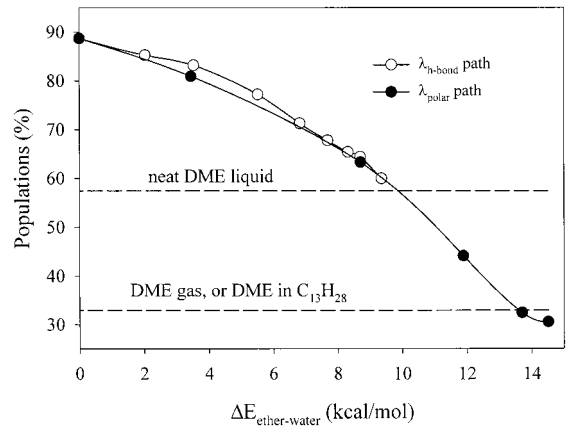

Figure 8. Hydrophilic conformation populations for DME at 298 K as a function of the parametric variable $\Delta E_{ether-water}$.

populations. The total hydrophilic population[7] of DME is shown as a function of $\Delta E_{ether-water}$ in Figure 8 for the λ_{polar} and λ_{h-bond} paths. The increasingly hydrophobic nature of the ether−water interactions with increasing $\Delta E_{ether-water}$ is reflected in a decreasing hydrophilic ether conformer population. Figure 8 also shows the DME conformer populations obtained from simulations in a n-$C_{13}H_{28}$ solvent as well as in the neat melt. The hydrophilic population of DME in the nonpolar n-$C_{13}H_{28}$ solvent is quite similar to that obtained in aqueous solution with nonpolar ether−water interactions ($\lambda_{polar} = 1.0$) and is also nearly identical to that obtained in gas-phase DME. Comparing populations in the neat melt, which is polar but non-hydrogen-bonding environment for DME,[20] with those for a polar aqueous solution

without ether−water hydrogen bonds ($\lambda_{h-bond} = 1.0$), we can see that the latter provides a more hydrophilic environment than the neat melt, consistent with the higher dielectric constant (dipole moment per unit volume) for water compared to DME.

On the basis of changes in DME populations in aqueous solution compared to those in a nonpolar environment (e.g., gas phase or n-$C_{13}H_{20}$), we can determine the relative excess free energy of solvation of hydrophilic and hydrophobic conformers using the relationship[3,8]

$$\Delta[\Delta G_{EX}] = -kT \ln\left(\frac{P_{water}}{1 - P_{water}} \frac{1 - P_{nonpolar}}{P_{nonpolar}}\right) \quad (6)$$

where P_{water} and $P_{nonpolar}$ are the hydrophilic conformer populations in water and nonpolar solvent, respectively. Using populations given in Figure 8, we find that hydrophilic DME conformers have a free energy of hydration that is 1.6 kcal/mol more favorable than for hydrophobic conformers, which is reflected in the increase in population of hydrophilic conformers in water relative to nonpolar solvents. The relative favor of hydrophilic conformers in solution decreases monotonically (i.e., their population decreases) with increasing hydrophobic character of the ether−water interactions, as revealed in Figure 8. For the DME solution with nonpolar ether−water interactions ($\lambda_{polar} = 1.0$) there is essentially no difference in free energy of hydration for hydrophilic and hydrophobic conformers, meaning the conformations are essentially unchanged from those in nonpolar solvents. By comparing hydrophilic DME populations in unperturbed water solution, in water without ether−water hydrogen bonds ($\lambda_{h-bond} = 1.0$), and in water without polar ether−water interactions ($\lambda_{polar} = 1.0$), we find through application of eq 6 that about 40% of the relative hydrophilicity (−1.6 kcal/mol) of hydrophilic DME conformers compared to hydrophobic is the result of polar effects exclusive of hydrogen bonding, and about 60% results from more favorable hydrogen bonding of water with hydrophilic DME conformers. Since in dilute aqueous solution about 85% of DME (and PEO) conformers are hydrophilic, and their free energy of solvation is 1.6 kcal/mol more favorable than that of hydrophobic conformers, about 1.5 kcal/mol or around 20% of the favorable effects (about 6.7 kcal/mol) of ether−water hydrogen-bonding and polar interactions on the free energy of solvation of DME can be attributed specifically to the hydrophilic nature of certain conformers. The remaining 80% of the favorable excess free energy of solution is independent of conformation. It is therefore unlikely that an increase in the population of local hydrophobic PEO conformations, which ranges from 15% (dilute solutions, low temperature) to around 60% (concentrated solutions, high temperature)[7] with temperature or composition is the primary driving force for the observed closed-loop phase behavior[21] of PEO−water solutions as has been suggested in commonly employed models for these solutions[22] and related polymer solutions such as Pluronics.[23]

VI. Summary

The role of ether−water hydrogen-bonding and electrostatic interactions on the solvation thermodynamics of the model PEO solution is summarized in Table 1, where excess properties for the unperturbed DME solution, the solution with nonpolar ($\lambda_{polar} = 1.0$) ether−water interactions, and the solution without ether−water hydrogen bonds ($\lambda_{h-bond} = 1.0$) are compared. Ether−water polar interactions strongly influence the excess free energy and enthalpy of solution, and about 60% of these effects can be attributed to ether−water hydrogen bonding. The entropy of hydration shows remarkably little change as ether−water interactions become significantly more hydrophobic through removal of ether−water hydrogen-bonding and polar interactions. The entropy gained by the removal of ether−water hydrogen bonds and restrictions on the alignment of hydrating waters due to ether−water polar interactions is offset by increased water structuring, particularly for oxygeneous hydration. Hence, while the free energy and enthalpy of hydration increase (become less favorable or more hydrophobic) smoothly from fully polar/hydrogen bonding ether−water interactions to completely nonpolar ether−water interactions, the entropy shows little change over the entire range of ether−water interactions investigated. We believe these trends will hold in general for aqueous soluble polymers, and not only in dilute solution: the free energy and enthalpy of solvation will depend on the detailed nature of the hydrogen-bonding and polar interactions between the polymer and water, which may, as in DME and PEO, depend on conformation, while the entropy of solvation will be nearly independent of these interactions and will depend primarily upon the volume of the solute, as can be seen by comparing DME and pentane (Table 1). The strong dependence of the excess free energy and entropy on the extent of ether−water hydrogen bonding, which our simulations have shown to change dramatically with temperature and composition in PEO−water solutions,[1] seems to imply that change in ether−water hydrogen bonding with temperature and composition is a more likely fundamental source of the complex phase behavior of PEO than changes in conformations. In future papers we will consider the thermodynamics of PEO oligomers in aqueous solution as a function of temperature, concentration, and PEO molecular weight.

Acknowledgment. The authors gratefully acknowledge support for this work from the National Science Foundation through Grant NSF DMR #0076306.

References and Notes

(1) Smith, G. D.; Bedrov, D.; Borodin, O. *Phys. Rev. Lett.* **2000**, *85*, 5583.
(2) *Poly(Ethylene Glycol) Chemistry: Biotechnical and Biomedical Applications*; Milton, J. H., Ed.; Plenum: New York, 1992. *Poly(Ethylene Glycol Chemistry): Chemistry and Biological Applications*; Milton, J. H., Ed.; American Chemical Society: Washington, DC, 1997.
(3) Smith, G. D.; Bedrov, D. *J. Phys. Chem. A* **2001**, *105*, 1283.
(4) Smith, G. D.; Jaffe, R. L.; Yoon, D. Y. *J. Phys. Chem.* **1993**, *97*, 12752.
(5) Smith, G. D.; Borodin, O.; Bedrov, D. *J. Comput. Chem.*, submitted.
(6) Jorgensen, W. L.; Chandrasekhar, J.; Madura, J. D.; Impey, R. W.; Klein, M. *J. Chem. Phys.* **1983**, *79*, 926.
(7) Smith, G. D.; Bedrov, D.; Borodin, O. *J. Am. Chem. Soc.* **2000**, *122*, 9548.
(8) Bedrov, D.; Smith G. D. *J. Phys. Chem. B* **1999**, *103*, 10001.
(9) Bedrov, D.; Smith, G. D. *J. Chem. Phys.* **1998**, *109*, 8118.
(10) Sharp, K. A.; Maden, B.; Manas, E.; Vaderhooi, J. M. *J. Chem. Phys.* **2001**, *114*, 1791.
(11) Ferrenberg, A. M.; Swendsen, R. H. *Phys. Rev. Lett.* **1989**, *63*, 1195.
(12) Müller, M.; Paul, W. *J. Chem. Phys.* **1994**, *100*, 719.

(13) Frenkel, D.; Smit, B. *Understanding Molecular Simulation: From Algorithms to Applications;* Academic Press: San Diego, 1996.
(14) Cabani, S.; Gianni, P.; Mollica, V.; Lepori, L. *J. Solution Chem.* **1981**, *10*, 563.
(15) Kusano, K.; Suurkuusk, J.; Wadsö, I. *J. Chem. Thermodyn.* **1973**, *5*, 757.
(16) Lüsse, S.; Arnold, K. *Macromolecules* **1996**, *29*, 4251.
(17) Dormidontova, E. *Macromolecules* **2002**, *35*, 787.
(18) $T\Delta S_{TRANS} = NkT \ln[V(\lambda)/V(\lambda=0)]$, where N is the number of molecules in the ensemble and V is the solution volume associated with a given value of λ_{polar} or λ_{h-bond}.
(19) Estimate error bars for the $T\Delta S$ are ±0.2 kcal/mol. Within these uncertainties, $T\Delta S$ (after subtracting of translational entropy changes) shows a clear decrease with increasing $\Delta E_{ether-water}$ for larger values of $\Delta E_{ether-water}$.
(20) Smith, G. D.; Jaffe, R. L.; Yoon, D. Y. *J. Am. Chem. Soc.* **1995**, *117*, 530.
(21) Saeki, S.; Kuwahara, N.; Nakata, M.; Kaneko, M. *Polymer* **1976**, *17*, 685. Bae, Y. C.; Shim, J. J.; Soane, D. S.; Prausnitz, J. M. *J. Appl. Polym. Sci.* **1990**, *47*, 471.
(22) Karlström, G. *J. Phys. Chem.* **1985**, *89*, 4962.
(23) Linse, P. *Macromolecules* **1993**, *26*, 4437.

MA011026T